



# A REVIEW ON CHARACTERISATION TECHNIQUES

*Neelam Rani<sup>b,\*</sup>, Karan singh gill<sup>a</sup>, Atul Jain<sup>b</sup>, Sonia Devi<sup>b</sup>*

*<sup>a</sup>G.G.J. Govt. College Hisar (Haryana)*

*<sup>b</sup> Government College Barwala, Hisar (Haryana)*

*\*Corresponding Author:*

***Dr Neelam Rani***

*Assistant Professor in Physics*

*Government College Barwala, Hisar (Haryana)*

## ABSTRACT

Characterization plays a pivotal role in understanding the structural, optical, mechanical, electrical, and nonlinear optical properties of crystalline materials. In recent years, single and polycrystalline materials have attracted significant attention due to their potential applications in optoelectronics, photonics, and nonlinear optical (NLO) devices. A comprehensive analysis of these materials requires the use of multiple complementary characterization techniques, each based on distinct physical and chemical principles. This review paper will give a brief introduction about various characterization techniques with fundamental physics/chemistry behind them. Various characterization techniques used in the present study are: (i) Powder X-ray diffractometer is used to find the structure of the grown crystals. (ii) High Resolution X-ray diffractometer is used to evaluate the crystalline perfection of the grown crystal. (iii) Spectroscopic methods (FTIR, NMR, PL, and UV-Vis-NIR) are used for qualitative and quantitative analyses of chemical compounds. (iv) The Impedance analyzer is used to measure the dielectric constant, dielectric energy loss of the grown crystals. (v) Vickers hardness tester equipped with a diamond square indenter is used to measure mechanical properties of the grown crystals. (vi) The Kurtz and Perry powder technique has been used to assess the relative second harmonic generation efficiency. (vii) Z-scan technique is used to determine the third harmonic of the grown crystals. (viii) Etching studies were done to reveal the dislocations in the grown crystal. (ix) Ion implantation was done to modify the physical property of the grown crystal and (x) Thermal studies were done to know the change in properties of the crystal with temperature. These techniques have been described in detail in the following section.

## 1. INTRODUCTION

The characterization of crystalline materials is a fundamental and indispensable component of materials research, as it provides the basis for understanding structure–property relationships that govern material performance in technological applications. In crystal growth studies, characterization techniques serve not only to confirm the successful formation of the desired phase but also to evaluate crystal quality, purity, stability, and functional properties. A comprehensive characterization approach is therefore essential for establishing the suitability of crystalline materials for applications in optoelectronics, photonics, and nonlinear optical devices [1,2].

Among the various characterization methods, X-ray diffraction techniques play a central role in structural analysis. Powder X-ray diffraction (PXRD) is widely employed to identify phase purity, crystal structure, and lattice parameters based on Bragg's diffraction principle, whereas high-resolution X-ray diffraction (HRXRD) provides detailed insight into crystalline perfection, lattice strain, mosaicity, and defect density. The combined use of PXRD and HRXRD enables a reliable assessment of both average structural features and subtle crystalline imperfections, which critically influence the optical and electronic behavior of crystals [3–6].

Spectroscopic characterization techniques are equally important for probing the chemical and electronic structure of crystalline materials. Fourier Transform Infrared (FTIR) spectroscopy is commonly used to identify functional groups and molecular vibrations arising from changes in dipole moment, while Nuclear Magnetic Resonance (NMR) spectroscopy offers atomic-level information on chemical environments and molecular configuration. Optical spectroscopic methods such as UV–Vis–NIR absorption spectroscopy and photoluminescence (PL) spectroscopy are essential for evaluating optical transparency, band gap energy, and emission characteristics, which are key parameters for photonic and optoelectronic applications [7–10].

Mechanical and electrical properties significantly affect the reliability and device integration of crystalline materials. Vickers Microhardness testing is a widely accepted method for evaluating mechanical strength, elastic–plastic deformation, and resistance to indentation, thereby providing insight into the mechanical stability of crystals. Dielectric characterization using impedance spectroscopy allows the determination of dielectric constant, dielectric loss, and frequency-dependent polarization mechanisms, which are crucial for understanding charge transport and energy storage behavior in dielectric and NLO materials [11–14]. Nonlinear optical characterization techniques are indispensable for assessing the potential of materials in frequency conversion and optical modulation applications. The Kurtz and Perry powder technique is a standard method for evaluating second harmonic generation (SHG) efficiency in non-centrosymmetric materials, while the Z-scan technique enables the determination of third-order nonlinear optical parameters such as nonlinear refractive index and nonlinear absorption coefficient. These techniques provide direct experimental evidence of nonlinear optical activity and are widely employed in the screening of new NLO materials [15, 16]. In addition to conventional characterization methods, ion irradiation has emerged as an effective approach for modifying and tailoring material properties through controlled defect introduction. Author reported Ion–matter interaction studies carried out using facilities such as the Low Energy Ion Beam Facility (LEIBF) at the Inter-University Accelerator Centre (IUAC), New Delhi, enable systematic investigation of irradiation-induced changes in structural, optical, and electrical properties of crystalline materials [17,18,37-38].The present review consolidates the fundamental principles, experimental methodologies, and significance of these characterization techniques as applied to crystalline materials. By highlighting their complementary roles and practical relevance, this article aims to provide a comprehensive reference framework for researchers engaged in crystal growth and functional material characterization

## 2. POWDER X-RAY DIFFRACTION

The X-ray diffraction is the unique scientific tool for the characterization of crystalline materials. With the introduction of X-ray Synchrotron source, X-ray technique has expanded well beyond their initial roll in structure determination. X-ray powder diffraction is used to determine the atomic structure of crystalline materials without the need for large ( $\sim 100 \mu\text{m}$ ) single crystals. The recorded X-ray powder diffraction pattern is used to identify the contents of the sample and to determine the presence or absence of any particular phase, the crystal structure of a new or unknown material, phase transitions and solid-state reactions, and internal strains etc. in the crystals. The photograph of the Bruker made D8 Advanced Powder Diffractometer, at National Physical Laboratory, New Delhi, is shown in Fig.1. The diffractometer is computer controlled having a goniometer of 435 mm diameter with minimum step size of  $0.005^\circ$ , parabolic graded multilayer mirror, graphite monochromator, scintillation detector and Cu target X-ray sealed tube to get  $\text{CuK}\alpha$  radiation. The system is powered with tension of 40 kV with current of 40mA. Radiation from an X-ray tube is collimated by a series of closely spaced parallel metal plates. These parallel plate combinations are known as solar slits. Increased resolution can be obtained by decreasing the separation between the metal plates of the collimator or by increasing the length of the

unit but this is achieved at the expense of intensity. The slits are usually, made of a metal with a high atomic number, such as molybdenum or tantalum (because of their high absorption capacities). The schematic representation of the diffractometer optics is shown in Fig.1(b). The diffractometer is computer controlled having Goniometer of 435 mm diameter with minimum step size of  $0.005^\circ$ , parabolic graded multilayer mirror, graphite monochromator, scintillation detector and Cu target X-ray sealed tube to get  $\text{CuK}\alpha$  radiation. The system is powdered with tension of 40 kV with current of 40 mA. Radiation from an X-ray tube is collimated by a series of closely spaced parallel metal plates. These parallel plate combinations are known as solar slits. The slits are usually, made of a metal with a high atomic number, such as molybdenum or tantalum (because of their high absorption capacities). Filter for common targets of X-ray tubes are listed as Mo, Cu, Cr and Pt. In the X-ray diffractometer, the X-ray detector is used for mainly three types, as proportional, scintillation and solid-state detectors. The angle between the plane of the specimen and the X-ray source is  $\theta$ , (Bragg angle). The angle between the projection of the X-ray source and the detector is  $2\theta$ . For this reason the X-ray diffraction produced with this geometry are often known as  $\theta/2\theta$  scan. In  $\theta/2\theta$  geometry the X-ray source is fixed and detector moves through a range of angles. The equipment can record the pattern from  $1^\circ - 167^\circ$  of  $2\theta$  with a speed of  $0.02^\circ/\text{sec}$ . The specimens with homogeneous particles size prepared by crushing the single crystals and sieving by a sieve were introduced sample holder. The diffraction patterns were recorded in  $\theta/2\theta$  diffraction mode. In an experiment, it is necessary scan the whole range of the detector angles. A choice of range depends on the crystal structure of the material (if known) but for unknown specimen, a large range of angles is often used because the positions of the reflections are not known.

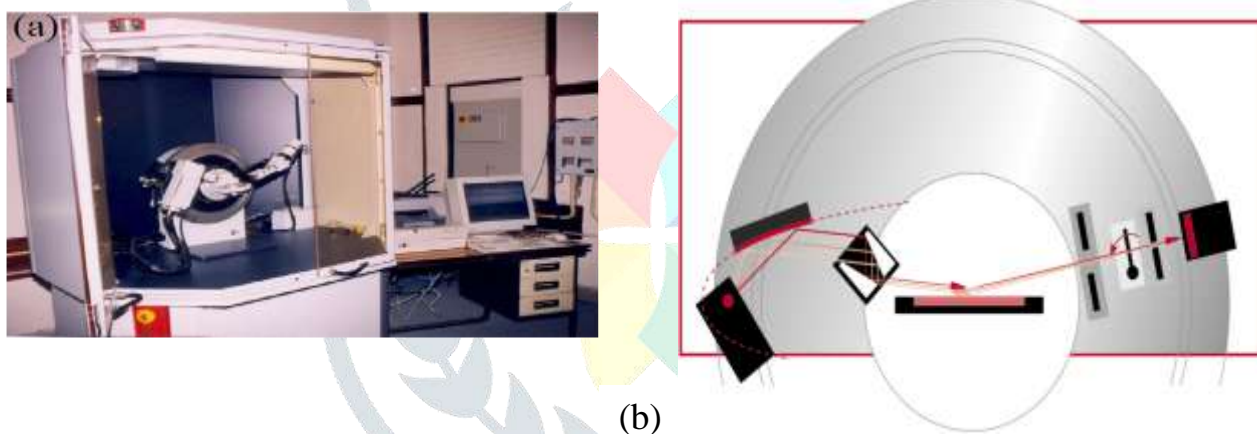


Fig.1: (a) Photograph of D8 advanced diffractometer, (b) Schematic representation of Diffractometer optics; (1). Goniometer (2). X-ray tube (3). Parabolic graded multilayer mirror (4). Graphite Monochromator (5). Sample holder (6). Soller slit (7). Detector assembly

### 3. HIGH RESOLUTION X-RAY DIFFRACTOMETER

As it is clear from the very beginning of the study of materials that their ability to perform <sup>7</sup> function was determined not only by the properties of the atomic elements composing it, But also by the interaction between them. In nature, the atoms/ions/molecules of material in solid state may be arranged in a random (as in amorphous or glassy material) or ordered (as in single crystal) way. The solid materials tend to be in the minimum energy state, which is possible in the perfect ordered state that is crystalline form. However, the conditions needed to form the material in the perfect crystalline state may be not achieved by the man. Therefore, the manmade crystals are expected to have defects in them. Basically, Point defect, Planar defects and Linear defects. The crystalline perfection of the grown single crystals was analyzed by the PANalytical X'Pert PRO MRD (Fig.2), high resolution XRD system having  $\text{CuK}\alpha_1$  radiation. The rocking curves have been recorded by  $\omega$  scanning. The monochromated X-ray beam ( $\text{CuK}\alpha_1$ ) incident on the specimen was obtained by using a hybrid 2-bounce Ge(220) monochromator with parabolic multilayer mirror assembly. The diffracted beam from the specimen was detected by using the scintillator detector with the triple axis 3-bounce Ge(220) analyzer crystal. This system is multipurpose and capable in

performing high-resolution X-ray diffractometry, high-resolution X-ray reflectometry (XRR), grazing incidence in plane XRD (GII-XRD) and reciprocal space mapping (RSM) for various technologically important nanostructures, such as epitaxial and amorphous multilayers, quantum wells, light emitting diode etc. The rocking curve for a single crystal can be recorded by changing the glancing angle around the Bragg diffraction peak position ( $\theta_B$ ) starting from a suitable arbitrary glancing angle ( $\theta_G$ ).

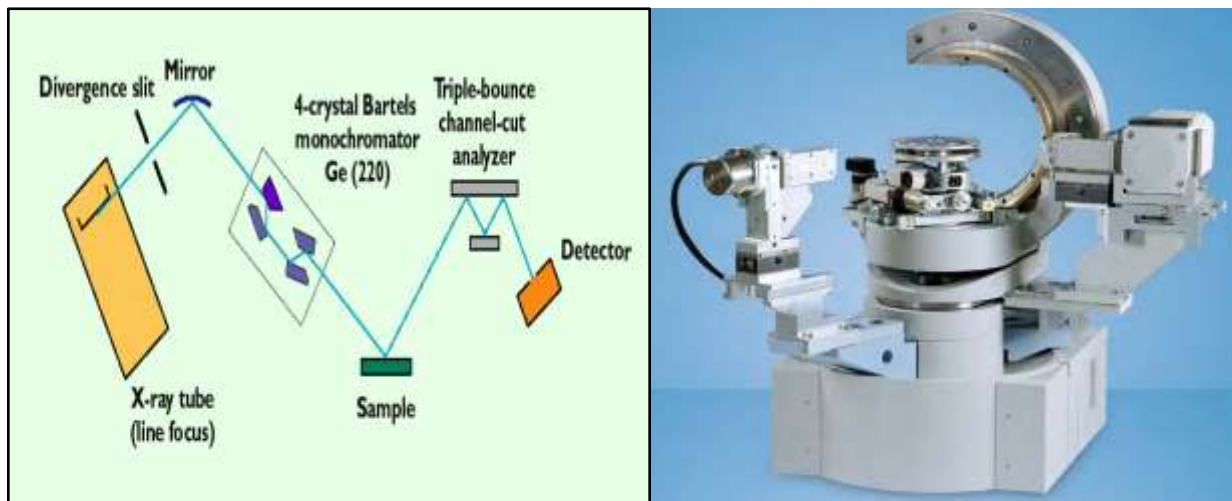


Fig.2: Schematic and Photograph of the multipurpose X'Pert PRO MRD PANalytical HRXRD cum XRR system

## 4. INFRARED SPECTROSCOPY

The instrument that determines the absorption spectrum for a compound is called an Infrared spectrometer. Two types of infrared spectrometers are in common use in organic laboratory: dispersive and Fourier transform (FT) instruments. Both of these types of instruments provide the spectra of the compounds in the common range of  $4000\text{cm}^{-1}$  to  $400\text{cm}^{-1}$ . Although two provides nearly identical spectra for a given compound, FT infrared spectrometer provides the infrared spectrum much rapidly than dispersive instruments. So FT-IR, is the preferred method of infrared spectroscopy. In infrared spectroscopy, IR radiation is passed through a sample. Some of the infrared radiation is absorbed by the sample and some of it is passed through (transmitted). In addition to the electronic transitions, the energy of a molecule can also change via rotational, vibrational, and vibronic (combined vibrational and electronic) transitions. These energy transitions often lead to closely spaced groups of many different spectral lines, known as spectral bands. Unresolved band spectra may appear as a spectral continuum. Infrared radiation is absorbed when a dipole vibrates naturally at the same frequency in the absorber. The pattern of vibrations is unique for a given molecule, and the intensity of absorption is related to the quantity of absorber. Thus, infrared spectroscopy permits the determination of components or groups of atoms that absorb in the IR-region ( $3 \times 10^{12}$  –  $3 \times 10^{14}$  Hz) at specific frequencies, permitting identification of the molecular structure. Like a fingerprint, no two unique molecular structures produce the same infrared spectrum. This makes infrared spectroscopy useful for several types of analysis. Simple diatomic molecules have only one bond which may stretch. More complex molecules have many bonds and vibrations can be conjugated leading to infrared absorptions at characteristic frequencies that may be related to chemical groups. For example, the atoms in a CH<sub>2</sub> group, commonly found in organic compounds can vibrate in six different ways: symmetrical and antisymmetrical, stretching, scissoring, rocking, wagging and twisting. Each molecule has certain natural vibrational frequencies. When infrared light is incident on the molecule, the frequency which matches the natural vibrational frequency is absorbed by the molecule resulting in molecular vibrations. Consequently, a change in dipole moment of the molecule occurs. There are two modes of vibration:

- (i) Stretching - distance between two atoms increases or decreases
- (ii) Bending - position of the atom changes relative to the original bond axis

IR technique works almost exclusively on samples with covalent bonds. IR absorption occurs as a result of vibrational and rotational transitions within the molecule. Because only a few compounds exhibit pure rotational bands, the vibrational absorption bands are of more practical interest. For a vibrational mode in a

molecule to be IR active, it must be associated with changes in the permanent dipole moment. IR spectroscopy helps in understanding the nature and types of bonds between two atoms which in turn helps in identifying the functional groups in a molecule on the basis of (i) strength of bonds based on vibration modes under IR radiation, and (ii) effective masses of two atoms forming a particular bond under investigation. The vibrational energy in wave number ( $\text{cm}^{-1}$ ) may be written as;

$$\nu = \frac{1}{2\pi c} \cdot \sqrt{\frac{k}{\mu}} \quad (1)$$

where,  $k$  is bond strength,  $\mu$  is the effective mass of the two bonded atoms and  $c$  is the speed of light. The photograph of the FT-IR is shown in fig.3.



**Fig.3:**Perkin Elemer GX 2000 FTIR spectrometer (at NPL, New Delhi)

A Schematic diagram of a dispersive infrared spectrometer is shown in Fig.4. The instrument produces a beam of infrared radiation and divides it into two parallel beams of equal intensity radiation by means of mirrors. The sample is placed into one beam and other beam is used as reference. The beam then passes into the monochromator, which disperse each into a continuous spectrum of frequencies of infrared light. The monochromator consists of a rapidly rotating sector (beam chopper) that passes the two beams alternatively to a diffraction grating varies the frequencies or wavelength of the radiation reaching the thermocouple detector. In this way, the detector determine the which frequency is absorbed by the sample and which frequency are unaffected by the light passing through the sample. Infrared radiation is produced by electrically heating a source, usually a Nernst filament or a Globar to  $1000 - 1800\text{ }^{\circ}\text{C}$ . Nichrome wire, carbon arc, rhodium wire and tungsten filament lamp are also used as light source. In a commercial infrared spectrometer either a nichrome wire or a platinum filament contained in a ceramic tube is commonly used as infrared source for the range  $4000 - 400\text{ cm}^{-1}$ . A monochromator is a means of separating wavelengths of the radiation source. Prisms and gratings are used for this purpose. A grating or a prism disperses the radiation from the source into its spectral elements. The monochromators perform three functions, which are basic to the operation of the instrument.

1. It disperses the radiation according to its wave number component.
2. It restricts the radiation falling on the detector into a narrow wave number range and
3. It maintains the energy incident on the detector to an approximately constant level when no sample is present throughout the wave number range of the instrument.

All infrared monochromator use mirror optics. Fortunately, the reflection from most metallic surfaces is good in the infrared region and consequently monochromator mirrors are normally worked in glass and finished with a thin reflecting coating of aluminum. The detector mostly produces an electrical signal which is proportional to the intensity of the incident radiation over the whole spectral range of the instrument. The most desirable features of the detectors are the closeness with which they approach the behaviour of a black body, high sensitivity, high speed and robustness. The infrared detectors may be selective or non-selective. The selective detectors are those whose response is markedly dependent upon the wavelength of the incident radiation. Examples of this type are photocells, Photographic plates, photoconductive cells and infrared phosphors. The non-selective detectors are those whose response is directly proportional to incident energy but relatively independent of wavelength. Common examples include thermocouples, bolometers and pneumatic cell. Recent detectors are fabricated from crystals such as lithium niobate, barium, titanate and triglycine sulphate. These crystals are known as pyroelectrics and take less time than other thermal detector. Hence with these crystals, radiation can be chopped at a higher

rate. However, these are more expensive and not widely employed. The radiant energy received by the detector is converted into measurable electrical signal and is amplified by the amplifiers. The amplified signal is registered by a recorder plotter. The recorder is driven with a speed which is synchronised with that of a monochromator, so that, the pen moving across the chart, records the transmittance of the sample as a function of the wave number.

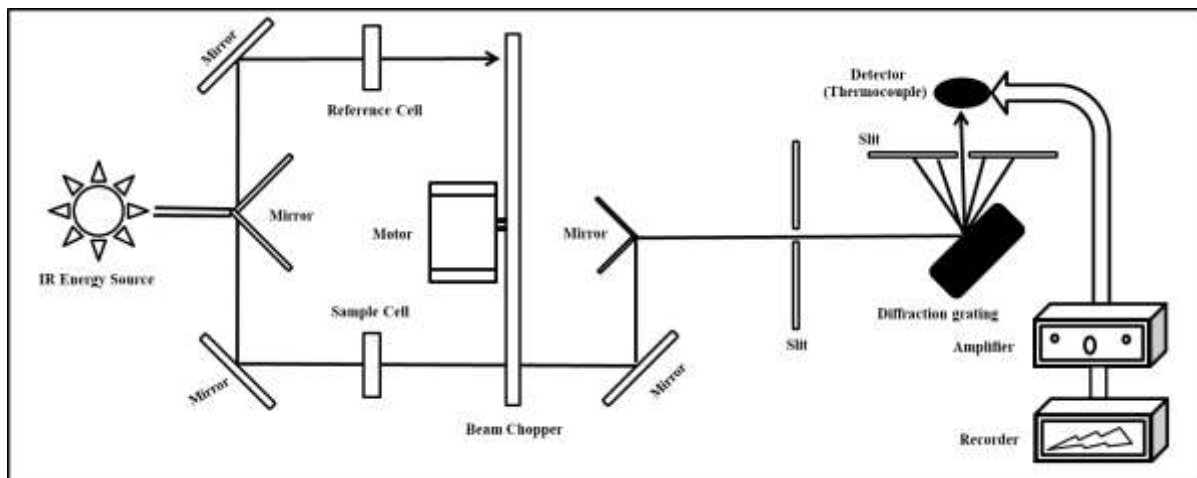


Fig.4. A Schematic diagram of a dispersive infrared spectrometer

## 5. NUCLEAR MAGNETIC RESONANCE (NMR) SPECTROSCOPY

Nuclear magnetic resonance (NMR) involves the interaction between an oscillating magnetic field of electromagnetic radiation and the magnetic energy of hydrogen nuclei when these are placed in an external magnetic field. The sample absorbs electromagnetic radiations in the radiowave region at different frequencies since absorption depends upon the type of protons or certain nuclei contained in the sample. The proton (circulating in orbit), as tiny magnetic bar precesses about the applied external magnetic field ' $H_0$ ' with precession frequency  $\omega$ , given by,  $\omega = \gamma H_0$ , where  $\gamma$  is the gyromagnetic ratio. The value of  $\gamma$  is given as ' $2\pi\mu/hI$ ' where  $\mu$  and  $I$  are the magnetic moment and spin quantum number of spinning magnet, and  $h$  is Plank's constant. The fundamental NMR equation is given by:

$$\gamma H_0 = 2\pi\nu \quad (2)$$

where,  $\nu$  stands for frequency of electromagnetic radiation. When a proton is placed in magnetic field, it starts precessing at certain frequency in radio-wave region by aligning along or against the field. The transition (flipping) of proton from one orientation to another can be brought by absorption of electromagnetic radiation in the radio-wave region of energy ' $h\nu$ '. In NMR spectroscopy the sample is kept under a constant radio-frequency signal and the strength of magnetic field constantly varied to get the transition condition.

The NMR is a unique technique for determining the structure of organic compounds. It is a powerful tool to reveal the number and nature of hydrogen and carbon atoms present in organic compounds [19]. The technique is helpful in assessing the overall molecular structure of a compound and is also useful for investigating variations in the electronic structure of crystals [20]. It deals with the magnetic properties of atomic nuclei having spin quantum number ( $I$ ) greater than 0:  $^1\text{H}$ ,  $^{13}\text{C}$ ,  $^{19}\text{F}$ ,  $^{31}\text{P}$ , etc., helps in recording differences in the magnetic properties of the various magnetic nuclei present and for deducing in large measures, the positions of these nuclei within the molecule [23]. It is possible to deduce how many different kinds of environments are there in the molecule for a particular atom and also which atoms are present in neighbouring groups. In a rigid molecule, it is possible for a proton to occupy a sterically hindered position and as a consequence, the electron cloud of the hindering group will tend to repel the electron cloud surrounding the proton. The proton will be deshielded and appear at higher delta ( $\delta$ ) values on the energy scale than would be predicted in the absence of the effect. Although this influence is small (usually less than 1 ppm), it must be born in mind when predicting the chemical shift positions in overcrowded molecules or macromolecules. Prediction of the  $^1\text{H}$  NMR spectrum of an organic compound begins with predicting the positions for the different hydrogen in the molecule.  $^1\text{H}$  NMR and  $^{13}\text{C}$  NMR are to obtain the chemical composition of the organic NLO single crystals grown with the organic dopants. The

idea and theory behind  $^{13}\text{C}$ -NMR is the same as with  $^1\text{H}$ -NMR, only the nucleus are different, are also recorded in the same way: Radio waves are used to study the energy level differences of nuclei.  $^1\text{H}$  and  $^{13}\text{C}$  nuclei have a nuclear spin of a half and thus have two energy levels. They can be aligned either with or against the applied magnetic field, as shown schematically in Fig. 5(a). A Bruker Advance III 400 NMR spectrometer Fig. 5(b), has been employed to investigate the structural variations in the single crystals lead due to the organic dopants by recording  $^1\text{H}$  and  $^{13}\text{C}$  spectra. The deuterated dimethylsulphoxide was used as solvent [5 ml for 5 mg] and spectrometer was operated at 400 MHz frequency by providing 16 and 1024 numbers of scan respectively for  $^1\text{H}$  and  $^{13}\text{C}$  spectra

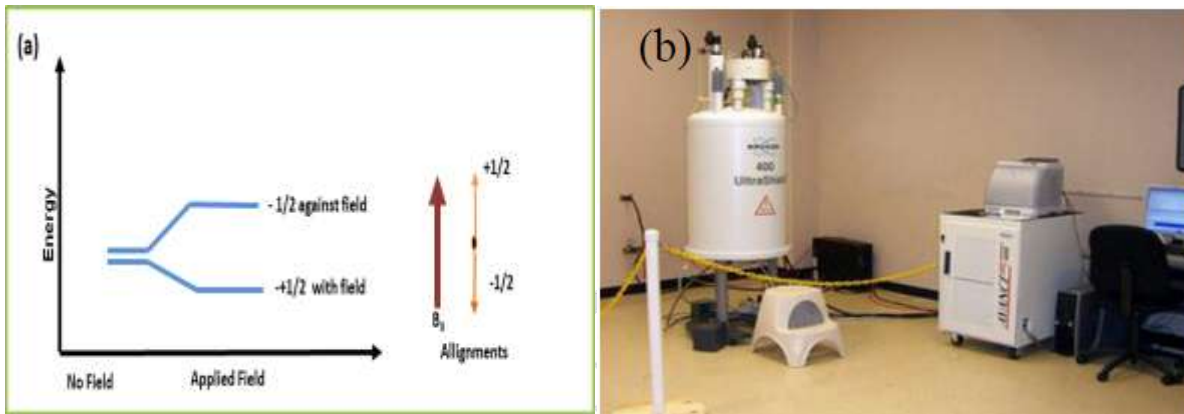


**Fig. 5:** The schematic indicating the splitting of the spin states of proton in absence and in presence of the applied magnetic field and photograph of the Bruker Advance III 400 NMR spectrometer

## 6. UV-VIS-NIR SPECTROSCOPY

Optical absorption is a very useful technique to study the metals, semiconductors, insulators in bulk, colloidal, nanostructures, thin films, etc. Optical absorption spectroscopy deals with the measurement of energy absorbed when electrons are promoted from ground state to higher energy levels. In the ground state, the spins of the electrons in each molecular orbital are essentially paired. In the higher state, if the spins of the electrons are paired then it is called an excited singlet state. On the other hand, if the spins of the electrons in the excited state are parallel, it is called excited triplet state. The electromagnetic radiation that is absorbed has energy exactly equal to the energy difference between the excited and ground states. The absorbed intensity is a function of the wavelength and useful in studying the electronic structure and transitions between the valance band and the conduction band of materials. The absorption of electromagnetic radiation in ultraviolet and visible wavelength region by an optical material is owing to the transition of electron in  $\sigma$  and  $\pi$  orbitals from ground state to higher energy states. The physical absorption in infrared and near infrared of the spectrum depends on the frequencies of atomic/molecular vibrations or chemical bonds. Inorganic materials contain only the covalent or ionic bonds, therefore exhibit higher transparency whereas, the organic materials possess multiple bonds, aromatic conjugation and different functional groups, hence suffer from the higher optical absorption with longer maximum wavelength of the absorption spectrum. The strength of electronic spectroscopy lies in its ability to measure the extent of multiple bond or aromatic conjugation within molecules or macromolecules, the longer the conjugation, longer the maximum wavelength of the absorption spectrum. The optical transparency of nonlinear optical materials is very important and for the device of single crystals, these must be having high optical transparency for a wide range of wavelengths. For this purpose a UV-VIS-NIR spectrometer (Shimadzu-UV 1601 PC) has been employed. The photograph and schematic representation for optical system of the spectrometer are shown in Fig.6. The functioning of this instrument is relatively straightforward as depicted in the schematic. A beam of light from a visible and/or UV light source (colored red) is separated into its component wavelengths by a prism or diffraction grating. Each monochromatic (single wavelength) beam in turn is split into two equal intensity beams by a half-mirrored device. One beam, the sample beam (colored magenta), passes through a small transparent container (cuvette) containing which may be a empty one in case the sample is being studied directly or a solution of the compound being studied in a transparent solvent. The other beam, the reference (colored blue), passes through an identical cuvette containing only the solvent or the specimen. In the reported papers to measure the transparency and

absorbance of the grown crystals the crystal wafers of suitable thickness were placed in the path of sample beam without keeping any reference sample in the path of reference beam. The intensities of these light beams are then measured by electronic detectors and compared. The intensity of the reference beam, which should have suffered little or no light absorption, is defined as  $I_0$ . The intensity of the sample beam is defined as  $I$ . Over a short period of time, the spectrometer automatically scans all the component wavelengths in the manner described. The ultraviolet (UV) region scanned is normally from 200 to 400 nm, and the visible portion is from 400 to 800 nm. In the present instrument the light source also covered the near infrared i.e. up to 1100 nm. Absorption may be presented as transmittance ( $T = I/I_0$ ) or absorbance ( $A = \log I_0/I$ ). If no absorption has occurred,  $T = 1.0$  and  $A = 0$ . Most spectrometers display absorbance on the vertical axis, and the commonly observed range is from 0 (100% transmittance) to 2 (1% transmittance).

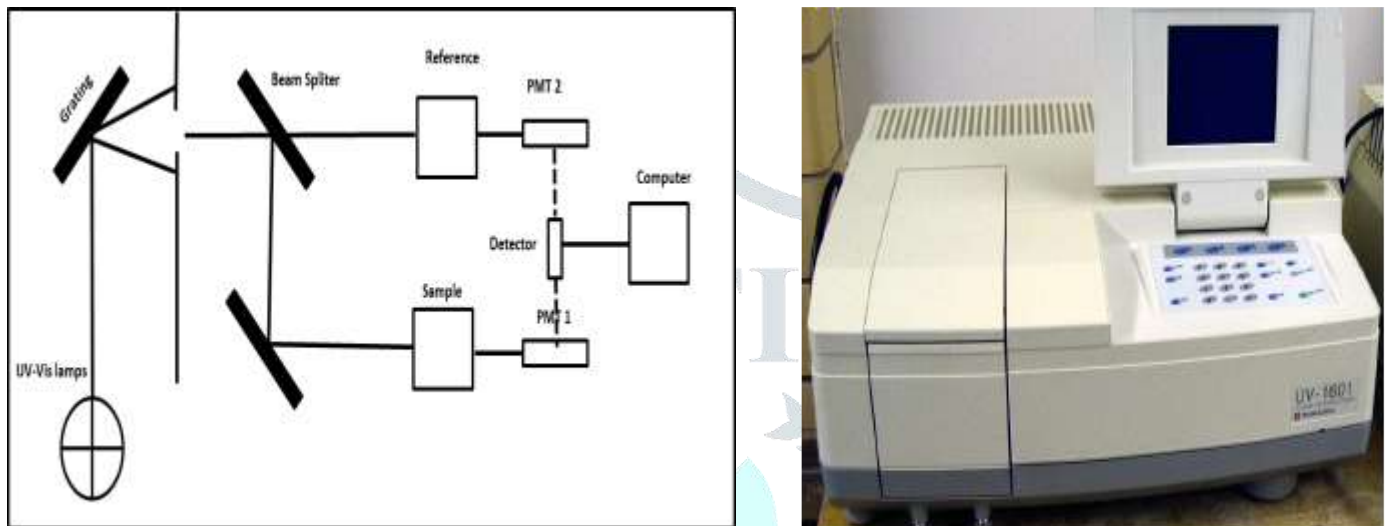


Fig.6: The schematic representation for optical system of the spectrometer and photograph of UV-VIS-NIR spectrometer (Shimadzu-UV 1601 PC at NPL, New Delhi)

## 7. PHOTOLUMINESCENCE SPECTROSCOPY

Photoluminescence (PL) is a process in which an atom absorbs a photon of light resulting in the transition to higher electronic energy state and emits photon while returns back to the lower energy state. It is a process whereby the matter generates non-thermal type of optical radiation usually in the visible range, but can also be in other spectral regions such as UV and IR. PL can be described as three step process: (1) absorption of excitation energy and stimulation of system into excited state, (2) transformation (from excited state to metastable state) and transfer of the excitation energy, and (3) emission of light or relaxation of the system to ground state. The spectral energy distribution and time dependence of the emission are related to electronic transition probabilities within the sample, and can be used to provide qualitative and, sometimes, quantitative information about chemical composition, structure (bonding, disorder, interfaces, quantum wells), impurities, kinetic processes, and energy transfer. Fig.7 shows a typical PL spectrometer from Edinburgh Instruments, (model F900). The spectrometer irradiates the sample using a Xenon lamp, which excites the sample and the PL emission intensity as a result of relaxation of the sample is measured as a function of wavelength. A typical configuration of the spectrometer is schematically described is shown in Fig.7. The excitation monochromator isolates a band of a particular wavelength from the light from the xenon lamp to excite the samples kept in the sample holder. The emission monochromator selectively receives fluorescence emitted from the sample and its photomultiplier (PM) tube measures the intensity of the fluorescence. The beam splitter is used to measure the intensity of incident or excitation radiation through the PM. Well prepared wafers of grown single crystals were subjected to the spectrometer to record the excitation and emission spectra and for all specimens the experimental conditions were kept identical. The cut-off filters were used to separate out the wavelength of excitation from the emission spectra reaching the photomultiplier tube.

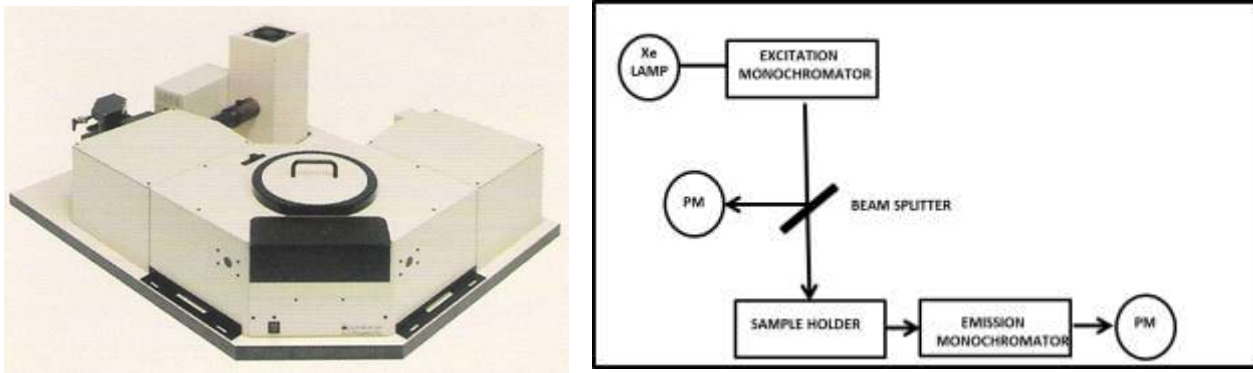


Fig.7. Photograph of PL (Edinburgh Instruments, (model F900)) spectrometer at NPL, New Delhi and the Schematic diagram of Photoluminescence Spectrophotometer

## 7. DIELECTRIC MEASUREMENTS

The dielectric constants of semiconductors are among the most important properties. Their magnitude and temperature dependence are important for both fundamental and applied considerations. These properties enter in an important way into the physics underlying the optical, transport and lattice-dynamical properties of semiconductors. They are also important in consideration of defects and impurity states. It is thus necessary to understand the dielectric properties and their temperature dependence in terms of the various mechanisms of dielectric polarisation. The real part of the dielectric constant ( $\epsilon_r$ ) is determined from the relation

$$\epsilon_r = \left(\frac{C}{C_0}\right) \quad (3)$$

Further, the capacitance of a parallel plate capacitor in air is given by

$$C_0 = \epsilon_0 \left(\frac{A}{d}\right) \quad (4)$$

where, 'A' is the cross-sectional area, 'd' is the thickness of the sample and ' $\epsilon_0$ ' is the permittivity of the free space and is equal to  $8.854 \times 10^{12}$  farad/meter.

By comparing the equation (3) and (4), we get

$$\epsilon_r = \left(\frac{d}{\epsilon_0 \cdot A}\right) \cdot C \quad (5)$$

Thus, by measuring the value of the capacitance, 'C' the value of dielectric constant (relative permittivity) can be found. The capacitance "C" is measured by PSM1735 impedance analyzer (Fig.8). By knowing the value of dielectric loss ( $\tan\delta$ ) with the help of above equipment, the ac electrical conductivity can be calculated using the formula

$$\sigma_{ac} = 2\pi f \cdot \epsilon_0 \epsilon_r \tan\delta \quad (6)$$

where  $f$  is the frequency of the applied ac signal. Thus, we find that like dielectric constant ( $\epsilon_r$ ), the dielectric loss ( $\tan\delta$ ) and ac electrical conductivity ( $\sigma_{ac}$ ) depend very much on frequency and temperature.



Fig.8. The Photograph of PSM1735 impedance analyzer at NPL, New Delhi

## 8. MICROHARDNESS

Hardness is a technique, in which a crystal is subjected to a relatively high pressure within a localized area. Hardness of a material is the resistance it offers to indentation. It may be termed as a measure of the resistance against lattice destruction or the resistance offered to permanent deformation or damage. The hardness properties are basically related to the crystal structure of the material. Microhardness study on the crystals brings out an understanding of the plasticity of the crystal. By suitable choice of indenter material and relatively simple equipment construction, hardness tests can be easily carried out on all crystalline materials under various conditions of temperature and pressure. Deformation is local, so that a number of trials can be made on a single specimen of small dimensions and can be reproduced by maintaining the specimen indenter orientation relationship. Specimen of flat relatively smooth surface is required. The Hardness measurement can be carried out by various methods, The Vicker's hardness test method is the most common and reliable method. In this method, micro indentation is made on the surface of a specimen with the help of diamond indenter (Fig.9). Smith and Sandland (Smith, 1923)[36] have proposed that a pyramid be substituted for a ball in order to provide geometrical similitude under different values of load. The Vickers pyramid indenter where opposite faces contain an angle ( $\alpha = 136^\circ$ ) is most widely accepted pyramid indenter. A pyramid is suited for hardness tests due to the following two reasons [24].

- (a) The contact pressure for a pyramid indenter is independent of indent size.
- (b) Pyramid indenters are less affected by elastic release than other indenters.

The base of the Vickers pyramid is square and the depth of indentation corresponds to  $1/7^{\text{th}}$  of the indentation diagonal. Hardness is generally defined as the ratio of the load applied to the surface area of the indentation. The Vickers hardness number ( $H_v$ ) of Diamond Pyramid Number (DPN) is defined as

$$H_v = \frac{2P \sin \alpha / 2}{d^2} \text{ kg/mm}^2 \quad (7)$$

where  $\alpha$  is the apex angle of the indenter ( $\alpha = 136^\circ$ ). The Vickers hardness number is therefore calculated from the relation

$$H_v = 1.8544P/d^2 \quad (8)$$

where  $P$  is the applied load in kg and  $d$  is the diagonal length of the indentation mark in mm. Hardness values are measured from the observed size of the impression remaining after a loaded indenter has penetrated and has been removed from the surface. Thus the observed hardness behaviour in the final measurement of the residual impression is the summation of a number of effects involved in the materials response to the indentation pressure during loading



Fig.9. Photograph of Vickers hardness (Make: Metatech, Pune) tester equipped with a diamond square indenter at NPL, New Delhi

## 9. KURTZ AND PERRY POWDER SHG TECHNIQUE

Nonlinear optics plays major role in photonics and optoelectronics. Extensive search for potential inorganic, organic and semiorganic nonlinear optical materials has been carried out. Powder SHG test offers the possibility of assessing the nonlinearity of the new materials. Kurtz and Perry proposed a powder SHG method for comprehensive analysis of the second order nonlinearity. This is an important method for characterization material before going through the long process of growing large optical quality crystals. The schematic diagram of Kurtz [22] powder SHG measurement is shown in fig.10. It consists of a Q-switched laser whose beam falls unfocused onto a thin section ( $\sim 0.2$  mm) of powder of the material under study. After the fundamental beam is removed by a series of short wavelength passing filters, the second harmonic is detected by a photomultiplier and displayed on an oscilloscope. A reference beam is obtained by use of beam splitter placed ahead of the sample. This enables the intensity of the fundamental or second harmonics generated in a reference sample [25] to be monitored by displaying both signals simultaneously on a dual-beam scope. The system also permitted the insertion of narrow-pass filters at the second-harmonic wavelength between the short filters and the photomultiplier to eliminate spurious signals. In order to improve the efficiency of second harmonic collection at the detector, a parabolic reflector was placed directly in front of the sample (that is, between the laser and the sample) with a small access hole for the laser beam. Nd:YAG laser of 1064 nm was used. It was Q-switched by a rotating mirror at a rate of 400 Hz. Peak powers in this case were  $\sim 1$  kW with pulse width of  $\sim 200$  ns [26,35].

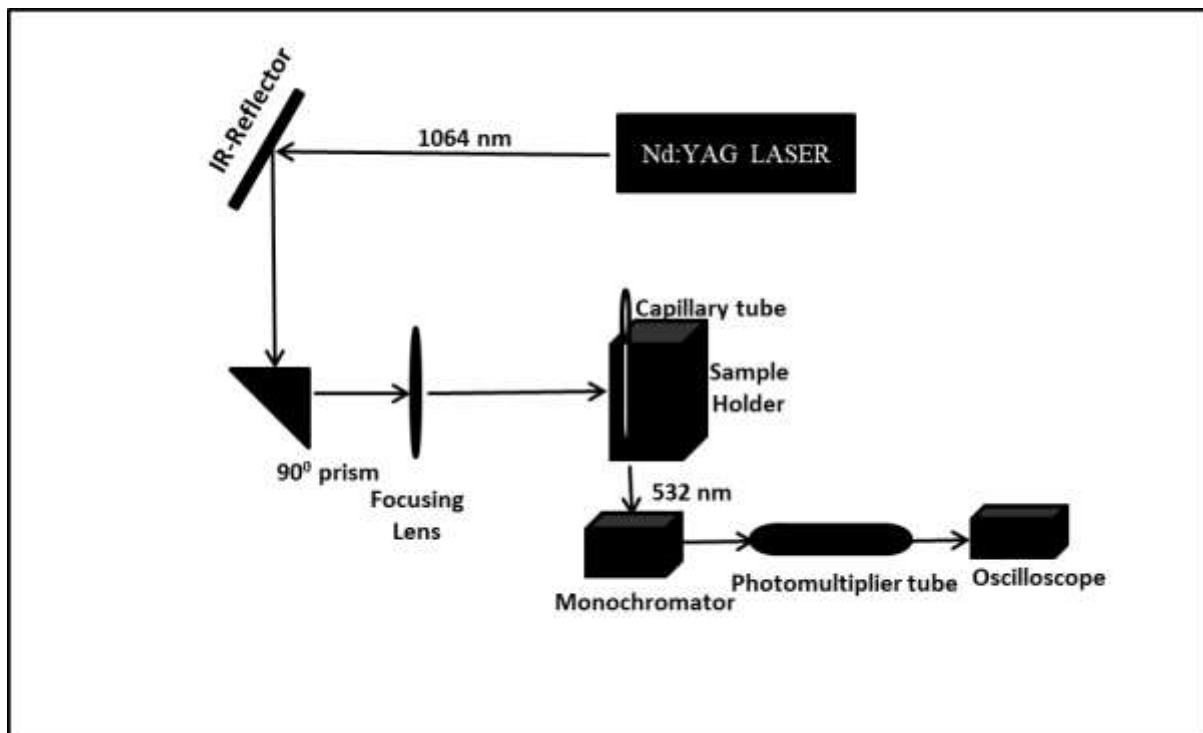


Fig.10. Schematic diagram of Kurtz and Perry powder SHG measurement technique

## 10. Z-SCAN TECHNIQUE

The Z-scan technique is a simple and sensitive single beam method to determine both the nonlinear refractive index and nonlinear absorption coefficient of materials. A Good complement to generate four-wave mixing(DFWM) is the Z-Scan technique, in that it can simultaneously measure the nonlinear absorption(NLA) and nonlinear refraction(NLR), which are related to imaginary and real parts of  $\chi^{(3)}$  respectively. Z-Scan is self focusing technique developed by Sheik-bahae et al. (1990) that involves focusing a laser beam through a thin sample and then detecting the light transmitted by a small aperture in the far field, in which the nonlinear act like an intensity dependent lens. The goal of a Z-Scan measurement is to obtain the aperture transmission as a function of sample position (Z) on the Z-axis. From the transmission curve, The magnitude, sign and real and imaginary parts of  $\chi^{(3)}$  are then extracted [28]. It is extremely sensitive and provides fast and clear results. Z-Scan can not measure off-diagonal elements of the susceptibility tensor and is greatly affected by beam shape, beam quality, sample distortions, and thermal effects. Furthermore, the beam comes to focus inside the sample, there is a significant possibility of damage of sample and sample holder at high light intensity. The sample causes an additional focusing and defocusing, depending on whether nonlinear refraction is positive or negative. The sensitivity to Nonlinear refraction is due to aperature, removal of the aperature completly remove this effect. This technique provides a highly sensitive straight forward method for determining the non-linear refractive index and non-linear absorption co-efficient of a large variety of materials by Andreas, 2004 [21]. A laser beam is focussed and transmittance through the sample is recorded as the position of the sample is varied relative to the focal length of the lens. A reference beam detector is used to monitor the fluctuation of the input. Z-scan is performed in two configurations with and without an aperture on the detector. Measurement with an aperture allows determination of sign and magnitude of the Kerr coefficient, while measurement with no aperture allows determination of sign and magnitude of two photon absorption. The block diagram of Z-scan technique is shown in fig.11.

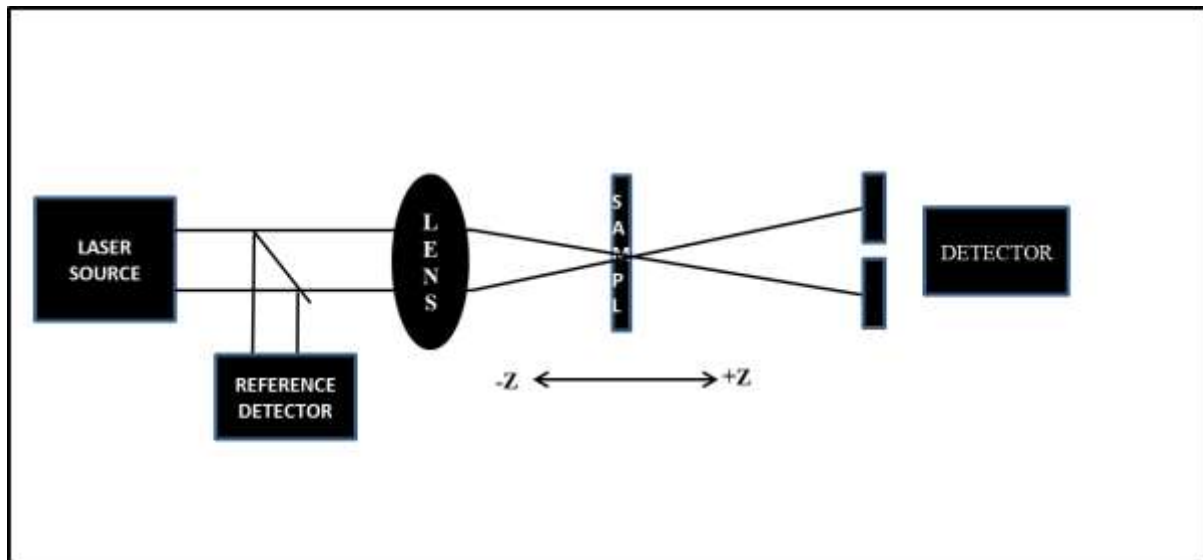


Fig.11. Schematic experimental Set up of Z-Scan

## 12. ETCHING STUDIES

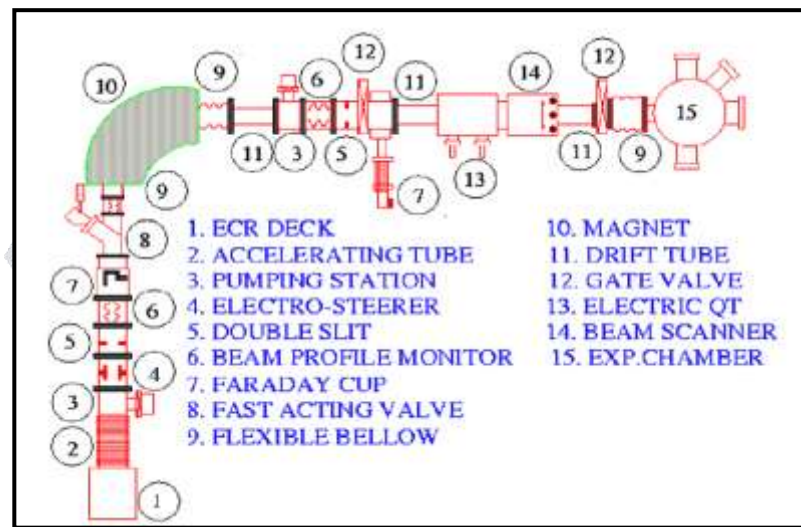
Crystals of better perfection are of demand for the use in the fabrication of electronic devices and in understanding the mechanism of plastic deformation. The etching studies reveal structural perfection and growth features of grown single crystals [29]. It is an important tool for the identification of crystal defects, which is able to develop some of the features such as growth hillocks, etch spirals, rectangular etch pits etc. on the crystal surface. The pattern of etch pits depend on the etchant, etching time and crystal faces. Etch pits are associated with dislocation and dislocation bundles and hence bring out the crystal quality [30]. The chemical etching study was carried out using double distilled water using Metatech optical microscope.

## 13. ION IMPLANTATION

Ion implantation is the process of surface or near surface modification of the composition of a material by controlled prelude of ions of an element. These ions are accelerated to energies in the range of tens of electron volts (eV) and a few MeVs and impinged on a solid. The interaction of ions with the target atoms results in their energy loss and the ions are finally stopped at a depth inside the material determined by their acceleration energy [34]. Virtually any element can be injected into the pre-determined region of any solid substrate. The process has been widely used in semiconductor doping during the last 40 years and is an integrated part of today's Si based VLSI technology. Ion implantation employs an ion implanter or a low energy ion beam accelerator consisting of an ion source, magnetic mass analyzer and an accelerating system. Inside a conventional implanter, a beam of positively charged ions is formed generally by injecting a gas into the ion source. The gas is ionized to form plasma. Ionization of the atom is performed for the purpose of acceleration. The ions are extracted from the source under high vacuum (pressures  $< 10^{-5}$  Torr) by applying an electrostatic field [31, 35]. Ion beam of solid materials is formed by using mainly sputtering method or by heating the solid near the melting temperature in a microwave oven.

The ion implantation was carried out at low energy ion beam facility (LEIBF), set up at IUAC, New Delhi [32, 33]. The facility is equipped with electron cyclotron resonance (ECR) based ion source placed on a high voltage (200 kV) platform. This source may provide high currents of multiply charged positive ions. A schematic diagram of the LEIBF facility is shown in Fig.12. Important parts of the facility are marked in the figure. Ions are produced inside the 10 GHz ECR source and extracted from it. All the components of the implanter including high power ultra high frequency transmitter, power supplies for extractor and einzel lens are placed on a high voltage deck (marked as 1) and controlled using optical fiber communication in multiplexed mode. The voltage difference between the high potential deck and the ground, distributed over the accelerating tube (marked as 2) grounded on the beam line end, provides ions at required kinetic energy. The vacuum inside extraction and accelerating

region is maintained below  $10^{-6}$  mbar through a pumping station, (3) constituted by a turbo pump backed by a rotary pump. Electrostatic steerer (4) and double slits (5) are used to steer the beam and to control the size of the beam, respectively. A beam profile monitor (BPM, 6) shows the distribution of the ions inside ion beam in two perpendicular (x- and y-) directions. Faraday cup (7) stops the beam whenever required. Valves (8, 12) usually provide isolation between two different sections of a beam line. Ions are mass analyzed using the magnet (10) and the required ions are selected by applying a particular value of magnetic field. Electric quadrupole-triplet (QT, 13) is used to focus the ions to desired location. During beam tuning, ion beam is focused in the shape of a fine circular spot. To provide a homogeneous implantation over the sample area, beam is electrostatically scanned using a beam scanner (14). Samples are mounted inside experimental chamber (15) on a copper ladder to provide an efficient heat flow from the samples generated as a result of impinged beam power. The pressure inside the experimental chamber is maintained in the low  $10^{-6}$  mbar regime. Ion implantation can be performed at any temperature between 80 K and 673 K in this chamber.



12. Schematic diagram of ECR ion source based LEIBF at IUAC, New Delhi

## 14. THERMAL ANALYSIS

Thermal analysis is a branch of material science where the properties of materials are studied as they change with temperature. Thermal analysis is also often used as a term for the study of heat transfer through crystal structures. We have employed three methods which are commonly used- these are distinguished from one another by the measured property;

### 14.1. THERMOGRAVIMETRIC ANALYSIS (TGA)

TGA is a method of thermal analysis in which changes in physical and chemical properties of materials are measured as a function of increasing temperature (with constant heating rate), or as a function of time (with constant temperature and/or constant mass loss). TGA can provide information about physical phenomena, such as second-order phase transitions, including vaporization, sublimation, absorption, adsorption, and desorption. Likewise, TGA can provide information about chemical phenomena including chemisorptions, desolvation (especially dehydration), decomposition, and solid-gas reactions (e.g., oxidation or reduction).

### 14.2. DIFFERENTIAL THERMAL ANALYSIS (DTA)

DTA is a thermoanalytic technique, similar to differential scanning calorimetry. In DTA, the material under study and an inert reference are made to undergo identical thermal cycles, while recording any temperature difference between sample and reference. This differential temperature is then plotted against time, or against temperature (DTA curve or thermogram). Changes in the sample, either exothermic or endothermic, can be detected relative to the inert reference. Thus, a DTA curve provides data on the transformations that have occurred, such as glass transitions, crystallization, melting and

sublimation. The area under a DTA peak is the enthalpy change and is not affected by the heat capacity of the sample.

### 14.3. DIFFERENTIAL SCANNING CALORIMETRY (DSC)

DSC is a thermo analytical technique in which the difference in the amount of heat required to increase the temperature of a sample and reference is measured as a function of temperature. Both the sample and the reference are maintained at nearly same temperature throughout the experiment. Generally, the temperature program for a DSC analysis is designed such that the sample holder temperature increases linearly as a function of time. The reference sample should have a well-defined heat capacity over the range of temperatures to be scanned.

Acknowledgement : The author gratefully express her sincere gratitude to the Director of National Physical Laboratory ,New Delhi and Director of IUAC, New Delhi for providing the facilities and support during the course of her research work.

## REFERENCES

1. Cullity, B. D., & Stock, S. R., *Elements of X-Ray Diffraction*, 3rd ed., Prentice Hall, New Jersey, USA, 2001.
2. Suryanarayana, C., & Norton, M. G., *X-Ray Diffraction: A Practical Approach*, Springer, New York, USA, 1998.
3. Warren, B. E., *X-Ray Diffraction*, Dover Publications, New York, USA, 1990.
4. Jenkins, R., & Snyder, R. L., *Introduction to X-Ray Powder Diffractometry*, John Wiley & Sons, New York, USA, 1996.
5. Lal, K., & Bhagavannarayana, G., "A high-resolution diffuse X-ray scattering study of defects in dislocation-free crystals," *Journal of Applied Crystallography*, **22**, 209–215 (1989).
6. Bhagavannarayana, G., Kushwaha, S. K., & Budakoti, G. C., "Characterization of crystalline perfection of single crystals by high-resolution X-ray diffraction," *Journal of Applied Crystallography*, **43**, 154–162 (2010).
7. Stuart, B., *Infrared Spectroscopy: Fundamentals and Applications*, John Wiley & Sons, Chichester, UK, 2004.
8. Macomber, R. S., *A Complete Introduction to Modern NMR Spectroscopy*, John Wiley & Sons, New York, USA, 1998.
9. Pankove, J. I., *Optical Processes in Semiconductors*, Dover Publications, New York, USA, 1971.
10. Lakowicz, J. R., *Principles of Fluorescence Spectroscopy*, 3rd ed., Springer, New York, USA, 2006.
11. Onitsch, E. M., "Über die Mikrohärte der Metalle," *Mikroskopie*, **2**, 131–151 (1947).
12. Meyers, M. A., & Chawla, K. K., *Mechanical Behavior of Materials*, 2nd ed., Cambridge University Press, Cambridge, UK, 2009.
13. Jonscher, A. K., *Dielectric Relaxation in Solids*, Chelsea Dielectrics Press, London, UK, 1983.
14. Macdonald, J. R. (Ed.), *Impedance Spectroscopy: Emphasizing Solid Materials and Systems*, John Wiley & Sons, New York, USA, 1987.
15. Kurtz, S. K., & Perry, T. T., "A powder technique for the evaluation of nonlinear optical materials," *Journal of Applied Physics*, **39**, 3798–3813 (1968).
16. Sheik-Bahae, M., Said, A. A., Wei, T. H., Hagan, D. J., & Van Stryland, E. W., "Sensitive measurement of optical nonlinearities using a single beam," *IEEE Journal of Quantum Electronics*, **26**, 760–769 (1990).
17. Srivastava, S. C., *Ion Beam Interactions with Matter*, Springer, New Delhi, India, 2012.
18. Avasthi, D. K., & Mehta, G. K., *Swift Heavy Ions for Materials Engineering and Nanostructuring*, Springer, Dordrecht, 2011.
19. Dani, V. R. (1995) 'Organic Spectroscopy' Tata McGraw-Hill, New Delhi.
20. Sharma, Y. R. (2000) *Elementary Organic Spectroscopy*, S. Chand Pub., New Delhi.
21. Andreas, B., Peithmann, K., Buse, K. & Maier, K. (2004) *Appl. Phys. Lett.* **81**, 3813-3815.

22. Kurtz S.K. and Perry T.T. (1968), 'Powder technique for the evaluation of nonlinear optical materials', J. Appl. Phys., Vol.39, pp.3798-3813.
23. Banwell, C.N. & McCash, E. M. (1994) Fundamentals of Molecular Spectroscopy, 4th Edition, New Delhi: Tata McGraw-Hill Publishing Company.
24. Calleja F. J. B., Mead W. T., Porter R. S., Polymer Engineering & Sci., 20 (1980) 393.
25. Ducuing J., Bloembergen N., Phys. Rev., 133 (1964) A1493.
26. Born G. V. R., *Nature*, 95 (1964) 202.
27. Sheik-Bahae M., Hagan D. J., IEEE J. Quantum electronics, 26 (1990) No. 4.
28. Kerns J. G., Berenbaum, Howard J. of Abnormal Psychology, 111 (2002) 211.
29. Kirupavathy S. S., Mary S. S., Srinivasan P., Vijayan N., Bhagavannarayana G., Gopalakrishnan R., J. Crystal Growth, 306 (2007) 102.
30. Devi T. U., Lawrence N., Babu R. R., Ramamurthi K., Bhagavannarayana G., Spectrochim. Acta A, 71 (2009) 1667.
31. Koivisto H., Arje J., Nurmi M., Rev. Sci. Instrum., 69 (1998) 785.
32. Kumar P., Rodrigues G., Rao U. K., Safvan C. P., Kanjilal D., Roy A., Pramana, J. Phys., 59 (2002) 805.
33. Kanjilal D., Madhu T., Rodrigues G., Rao U. K., Safvan C. P., Roy A., Int. J. Pure and Appl. Phys., 25 (2001) 39.
34. Ziegler J. F., Biersack J. P., Littmark U., Pergamon Press, New York, (1985).
35. Wolf B., Taylor and Francis, CRC Press, Australia, (1995).
36. R.L. Smith and G.E. Sandly, Proc. Inst Mech Eng., (1922).

